Transactions, SMiRT-25
Charlotte, NC, USA, August 4-9, 2019
Division III

EFFECT OF NON-VERTICALLY PROPAGATING EARTHQUAKE WAVES AND NONLINEAR SOIL-STRUCTURE INTERACTION ON NUCLEAR FACILITY RESPONSE

Swetha Veeraraghavan[1], Justin Coleman[2]

[1] Computational Research Scientist, Idaho National Laboratory, Idaho Falls, ID, USA (swetha.veeraraghavan@inl.gov)
[2] Senior Technical Advisor Microreactors, Idaho National Laboratory, Idaho Falls, ID, USA

ABSTRACT

Most of the existing nuclear power plants are founded close to the soil surface. Previous studies have demonstrated that surface-founded structures exhibit increased rocking and torsional responses when subjected to non-vertically propagating seismic waves. However, in most of these studies the base of the structure was assumed to be tied to move with the soil surface. Recently, Bolisetti et al. (2015) demonstrated that geometric nonlinearity, i.e., gapping, sliding and uplift of the structure with respect to the soil can significantly alter the response of a surface-founded structure when subjected to vertically propagating seismic waves. The current study aims at understanding the effect of geometrically nonlinear soil-structure interface behaviour on the response of a surface-founded structure subjected to obliquely incident seismic waves. A stick-mass model of a representative nuclear power plant connected to a stiff basemat is used for this study. Four different soil-structure interface conditions and 3 different earthquake fault rupture scenarios are considered for this study. The preliminary results from these studies suggest that the addition of geometrically-nonlinear interface reduces the response of the structures in the horizontal direction and decreases the natural frequency of the system in the vertical direction when subjected to inclined seismic waves.

INTRODUCTION

Seismic response of nuclear power plants has been an area of active research for many decades. One of the common assumptions involved in the analysis of nuclear power plants is that the seismic waves are vertically incident on the structure. This assumption is valid when the earthquake fault is located far from the structure. However, if an earthquake fault is discovered close to an existing nuclear facility, the waves generated from the rupture of this fault would not necessarily be vertically incident on the structure. So, it is important to analyse the response of these structures to obliquely incident seismic waves.

Many researchers analysed the response of surface-founded structures to non-obliquely incident seismic waves under the assumption that the base of the structure is tied to move with the soil (for e.g., Thau and Umek, 1973; Wong and Luco, 1978; Luco and Wong, 1982). The results from these studies suggest that inclined shear vertical (SV), compressive (P) and Rayleigh waves cause increased rocking response of the structure, whereas inclined shear horizontal (SH) and Love waves result in increased torsional response of the structure.

Bolisetti et al. (2015) demonstrated that including just geometric nonlinearity, i.e., gapping, sliding and uplift of the structure with respect to the soil can significantly alter the in-structure response under vertically propagating seismic waves. In particular, the addition of geometric nonlinearity reduced the

horizontal acceleration response of the structure at frequencies less than 10 Hz but amplified the response at high frequencies. Since the main aim of this study was to understand the effect of soil-structure interface conditions, the nuclear power plant structure was modelled using a simplified stick-mass representation.

Since geometric nonlinearity plays a significant role even when the structure is subjected to vertically propagating waves, it is important to understand how geometric nonlinearities affect the response of a structure subjected to obliquely incident waves SV or P waves or Rayleigh waves, where the structure has a higher tendency to rock. In this study, the response of the idealized stick-mass nuclear power plant structure considered by Bolisetti et al. (2015) is modelled under obliquely incident quasi-plane seismic waves generated by the rupture of earthquake faults with three different fault inclinations. Additionally, four different soil-structure interface conditions are considered – tied interface and an interface that allows for uplift and sliding of the structure with respect to the soil with friction coefficients of 0.55, 0.7 and 0.9. The earthquake fault rupture, wave propagation from the fault to the site, and the nonlinear response of the soil-structure interface are all modelled using the open-source time domain finite element tool MASTODON (Coleman et al., 2017) developed at the Idaho National Laboratory.

MODEL DESCRIPTION

Structure Model

The nuclear power plant structure selected for this study is representative of a pressurized water reactor building and is obtained from the SASSI2000 user manual (Ostadan, 2006). The containment structure and the internal components are idealized using a stick-mass model as shown in Figure 1. The section properties of the different constituent beams and the values of the lumped masses are also presented in this figure. The Young's modulus for the massless beams representing the containment and internal structures are assumed to 1.026 GPa and 0.513 GPa, respectively, and the Poisson's ratio is assumed to be 0.278 for all the beams. Each of these sticks are discretized into 10 C0-Timoshenko beam elements for the finite element simulation.

The stick-mass model of both the containment and the internal structures are connected to a stiff 40 m x 3 m rectangular basemat with Young's modulus, Poisson's ratio and density of 14364 GPa, 0.3, and 2402 kg/m^3, respectively. The basemat is discretized using QUAD4 finite elements with a width of 7.5 m and height of 3 m. To avoid focusing the entire weight of the structure at the center of the basemat, stiff massless horizontal beams with Young's modulus and Poisson's ratio of 1436 GPa and 0.3, respectively, are used to connect the bottom node of the stick-mass models to the nodes on the top surface of the basemat. The first few natural frequencies of the finite element model are 5.26 Hz, 8.42 Hz, 12.21 Hz and 15.35 Hz. These frequencies match within 2% of those obtained using CLASSI and LS-DYNA that are presented by Bolisetti et al. (2015).

Soil-structure Model

To simulate non-vertically propagating earthquake waves through the rupture of inclined earthquake faults, a 2D linear anelastic homogenous soil domain that is 11 km x 8 km is considered for this study (Figure 2 (a)). The shear modulus of the soil is 1.7 GPa, Poisson's ratio is 0.3, and density is 1700 kg/m^3, resulting in a shear and compressive wave velocity of 1000 m/s and 1870.9 m/s, respectively. Compared with the large soil domain, the dimensions of the structure (located at the center of the soil domain on the free-surface) are only 40 m x 70 m. Thus, the presence of the structure would only affect the response of the soil very close to the structure (within ~ 5 x width of the basemat = 200 m). Therefore, simulating the entire 11 km x 8 km for every change in the basemat-soil interface condition is computationally inefficient.

The domain reduction method (DRM) developed by Bielak et al. (2003) is employed to improve computational efficiency in this scenario by splitting the computation into two separate steps. In the first

step, the free-field response of the large soil domain (without structure) is computed in response to the three different earthquake fault rupture scenarios (Figure 2(b)). In the second step, the results from the first step along the DRM layer are transferred as input to a much smaller computational domain containing the structure and a small region of soil around it (Figure 2(c)). The advantage of this method is that the large 11 km x 8 km computational domain would have to be simulated only thrice, once for each inclined fault. Only the smaller computational domain has to be re-simulated to study the effect of changes in the soil-structure interface conditions. More details about this method's implementation in MASTODON can be found in Veeraraghavan et al. (2017). The formulation and solution of the first part, i.e., the free-field response of the large soil domain subjected to inclined fault rupture, is discussed in detail in Veeraraghavan et al. (2017) and only a short discussion about the resulting wavefronts is provided in the next paragraph.

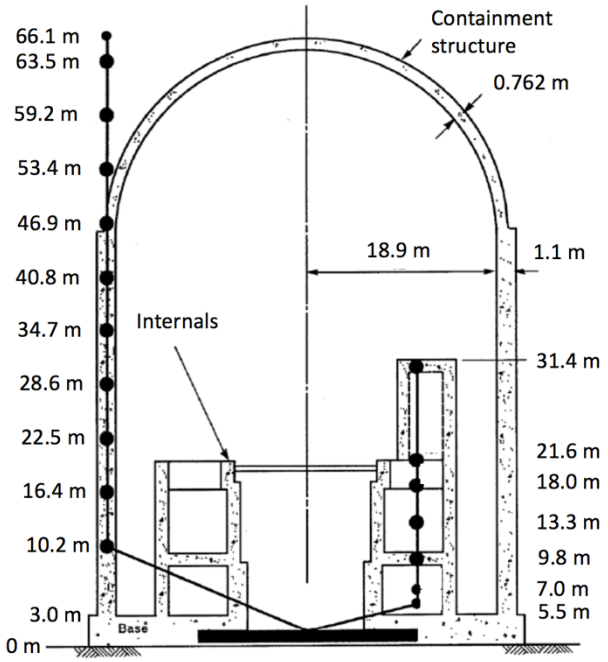

Containment structure

Elevation (m)	Mass (kg)	Area (m^2)	Shear Area (m^2)	Moment of Inertia (m^4)
10.2	6.4800E+04	130.0643	65.03215	2.4167E+04
16.4	5.9162E+04	130.0643	65.03215	2.4167E+04
22.5	5.9162E+04	130.0643	65.03215	2.4167E+04
28.6	5.9162E+04	130.0643	65.03215	2.4167E+04
34.7	5.9162E+04	130.0643	65.03215	2.4167E+04
40.8	5.9162E+04	130.0643	65.03215	2.4167E+04
46.9	6.4941E+04	130.0643	65.03215	2.4167E+04
53.4	4.2542E+04	91.974	46.44687	1.6399E+04
59.2	3.4795E+04	91.974	46.44687	1.2946E+04
63.5	2.9865E+04	91.974	46.44687	6.9048E+03
66.1	2.6762E+03	91.974	46.44687	1.7262E+03

Internal structure

Elevation (m)	Mass (kg)	Area (m^2)	Shear Area (m^2)	Moment of Inertia (m^4)
5.5	3.9444E+04	185.8061	92.90305	9.4941E+03
7	3.5358E+04	237.8318	118.9159	1.0357E+04
9.8	8.8605E+04	205.3157	102.65785	1.0357E+04
13.3	5.2966E+04	182.09	91.045	1.1220E+04
18	1.2030E+05	161.6513	80.82565	7.7679E+03
21.6	1.7187E+04	72.4644	36.2322	1.7262E+03
31.4	1.1553E+04	17.6516	8.8258	3.4524E+01

Figure 1. Stick-mass model of a representative nuclear power plant (left) along with properties of the beams and lumped masses (right). Adapted from SASSI 2000 user manual.

Snapshots illustrating the free-field velocity response of the large soil domain for the three different fault dips are presented in Figure 3. To enable direct comparison between these three scenarios, the results from the simulations in Veeraraghavan et al. (2017) are linearly scaled such that the maximum magnitude of velocity at the center of the soil domain is 1.83 m/s in all three scenarios, which is the maximum velocity recorded at Rinaldi station during the 1994 Northridge earthquake. In the case of the horizontal fault (Figure 3 (a)), a vertically propagating SV wavefront (red contour line) is generated and this wavefront on interaction with the free-surface is reflected back as a downward traveling SV wavefront. Therefore, majority of the wave energy in this scenario is in the horizontal direction. In both the 15° and 55° fault dip scenarios, inclined SV wavefronts are generated. When the 15° SV wavefront interacts with the free-surface, it is partially reflected back as an inclined SV wavefront and the rest of it is reflected as a P wavefront. In contrast, the 55° SV wavefront on interaction with the free-surface is partially reflected back as an inclined SV wavefront and the rest of the energy travels along the free-surface as a Rayleigh wave. Due to these inclined wavefronts and the resulting wave mode changes on interaction with the free-surface,

the free-surface response for the 15° and 55° scenarios are significantly different from that for the 0° scenario.

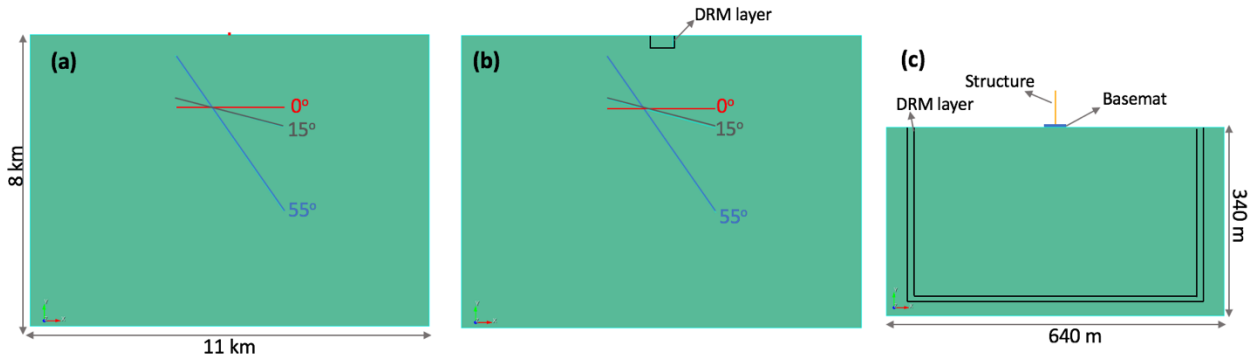

Figure 2. (a) A 2D 11 km x 8 km homogeneous soil domain with three different inclined earthquake faults and the structure located at the center of the free-surface. (b) Schematic of the soil domain with earthquake faults but without the structure, required for the first part of the DRM. (c) Schematic showing the smaller soil domain that contains the basemat and the structure for the second part of the DRM. The transfer of the information from (b) to (c) occurs along the DRM layer.

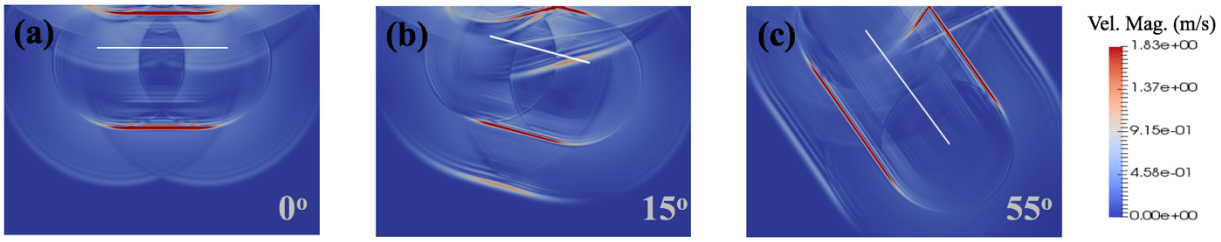

Figure 3. Snapshots showing contours of the velocity magnitude for (a) 0°, (b) 15° and (c) 55° earthquake fault dips. The white lines in these figures represent the earthquake fault and the red contour lines represent the main SV wavefront.

As mentioned in the previous paragraphs, the results from the free-field simulation are transferred to the smaller soil-structure computational domain along the DRM layer shown in Figure 2(c). 10 m x 10 m QUAD4 elements are used to mesh this soil domain and a timestep of 0.01 s is used for the simulation, which allows for accurate numerical wave propagation up to a maximum frequency of 10 Hz. To model the effect of geometric nonlinearity, i.e., gapping, sliding and uplift between the structure and the soil, three different interface conditions are considered with friction coefficients of 0.55, 0.7 and 0.9. A node-to-surface contact formulation is used to model the soil-structure interface in the finite element model with the nodes on the bottom surface of the basemat serving as the slave nodes and the top surface of the soil serving as the master surface. A scenario where the structure is tied to move with the soil is also modelled, and the results from this scenario serve as the baseline response.

Lsymer dampers (Lsymer, 1969) are placed at the left, right and bottom boundaries in Figure 2 (c) to simulate absorbing boundary conditions that allow waves generated from the soil-structure interaction to radiate out of the computational domain. This poses a challenge in initializing the response of the system to gravity as the displacements at these outer boundaries cannot be set to zero. To initialize the state of the system under gravity, a separate model is simulated where the left and right boundaries are fixed in the X

direction and the bottom boundary is fixed in the Y direction (Figure 4(a)). The steady-state reaction forces at these boundaries are then transferred as boundary condition to the soil-structure model and the values of the steady-state solution throughout the model are used as initial condition. So, in addition to absorbing boundary condition, reaction forces are also applied at the left, right and bottom boundaries in Figure 2(c) to equilibrate the system under gravity.

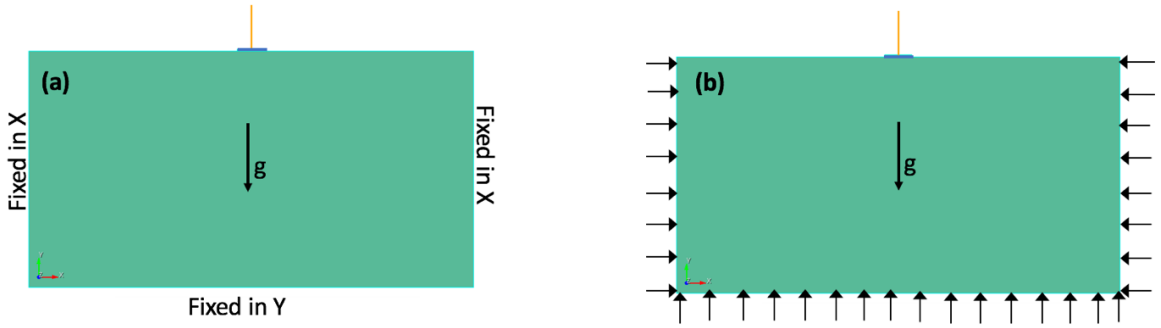

Figure 4. (a) Soil-structure model with fixed left, right and bottom boundaries to model response of the system under gravity. (b) The steady-state reaction forces at the left, right and bottom boundaries and the solution variables from (a) are then transferred as boundary and initial condition, respectively, to equilibrate the system under gravity without the use of kinematic boundary conditions.

RESULTS

The response of the structure is analysed under the 3 three different fault rupture scenarios for four different soil-structure interface conditions – tied and geometrically nonlinear interface with friction coefficients of 0.55, 0.7 and 0.9. To understand the effect of geometric nonlinearity, the spectral accelerations in the X and Y directions at the center point on the top surface of the basemat (also the base node of the structure) are presented in Figure 5 for the three different fault rupture scenarios and the 4 different soil-structure interface conditions.

For the horizontal fault (Figure 5(a)-(b)), the spectral acceleration in the vertical direction is negligible when compared to the horizontal direction, as the majority of the wave energy is carried by vertically propagating shear waves in this scenario. In the horizontal direction, the spectral acceleration is much lower for the scenarios where the basemat is allowed to slide in comparison to the tied interface condition. This shows that a significant portion of the energy is dissipated through the sliding mechanism. Also, as expected, the spectral acceleration increases with an increase in friction coefficient. These results agree well with the results presented by Bolisetti et al. (2015) for frequencies less than 10 Hz. However, for frequencies above 10 Hz, Bolisetti et al. (2015) reported higher response in the geometrically nonlinear scenarios compared to the tied interface scenario due to rocking and impact of the structure on the soil. Since the finite element size and time step used for this study can only guarantee accurate numerical wave propagation up to 10 Hz, the spectral acceleration results from this study are truncated at 10 Hz. A finer mesh and time step discretization is required to capture these higher frequency effects.

In both the 15° and 55° fault dip scenarios (Figure 5 (c)-(f)), the effect of geometric nonlinearity in the horizontal direction is similar to that for the 0° fault dip scenario, with the exception that the difference between the tied and sliding interface results is much lower in the 55° scenario compared to the other two fault dip scenarios. This is likely due to the relatively low amplitude of horizontal acceleration in the 55° dip scenario that results in smaller sliding displacements of the structure. In contrast, the response in the vertical direction in both the 15° and 55° scenarios are very different from the 0° fault dip scenario.

Compared to the tied interface response, the vertical response due to the geometrically nonlinear interface is higher at frequencies between 0.8-5 Hz and lower in the 5-10 Hz frequency range (Figure 5(d) and (f)). This may be due to a decrease in the natural frequency of the system because of the additional flexibility resulting from the basemat separating from the soil in the vertical direction. Also, the amplified response in the vertical direction in Figure 5 (f) for the cases with geometric nonlinearity may be attributed to larger rocking response of the basemat when it is allowed to separate from the soil compared to the case where it is tied to the soil. Additionally, the vertical acceleration corresponding to the three different friction scenarios are very similar, implying that the vertical response is due to the gapping and uplift of the basemat and is not affected by sliding.

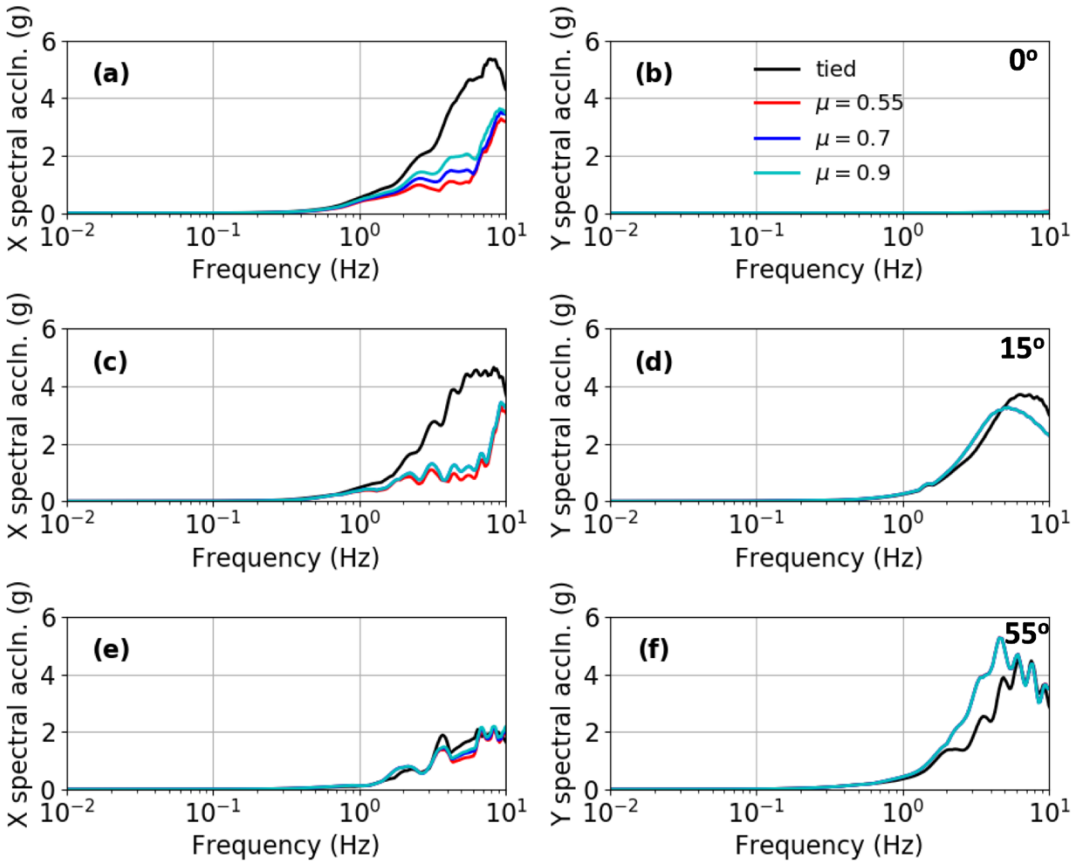

Figure 5. Spectral acceleration at the top of the basemat as a function of frequency in the horizontal and vertical directions for the three different earthquake fault dip scenarios and the four different soil-structure interface conditions. The left and right columns contain horizontal (X) and vertical (Y) spectral accelerations, respectively, and the first, second and third rows contain results for the 0°, 15° and 55° fault dips, respectively. The results for the different interface conditions are shown by the 4 different curves in each subfigure.

To understand the differences in the response of the structure due to the various source and interface conditions, the horizontal and vertical spectral accelerations of the lumped mass located 9.8 m above the soil surface are presented in Figure 6. The effect of geometric nonlinearity and inclined seismic waves on the response of this lumped mass is similar to that observed in the response of the basemat. In the horizontal direction, addition of geometric nonlinearity reduces the response, whereas in the vertical direction there is

small shift in the natural frequency of the system making it sensitive to seismic waves with a different frequency content than the system with tied interface.

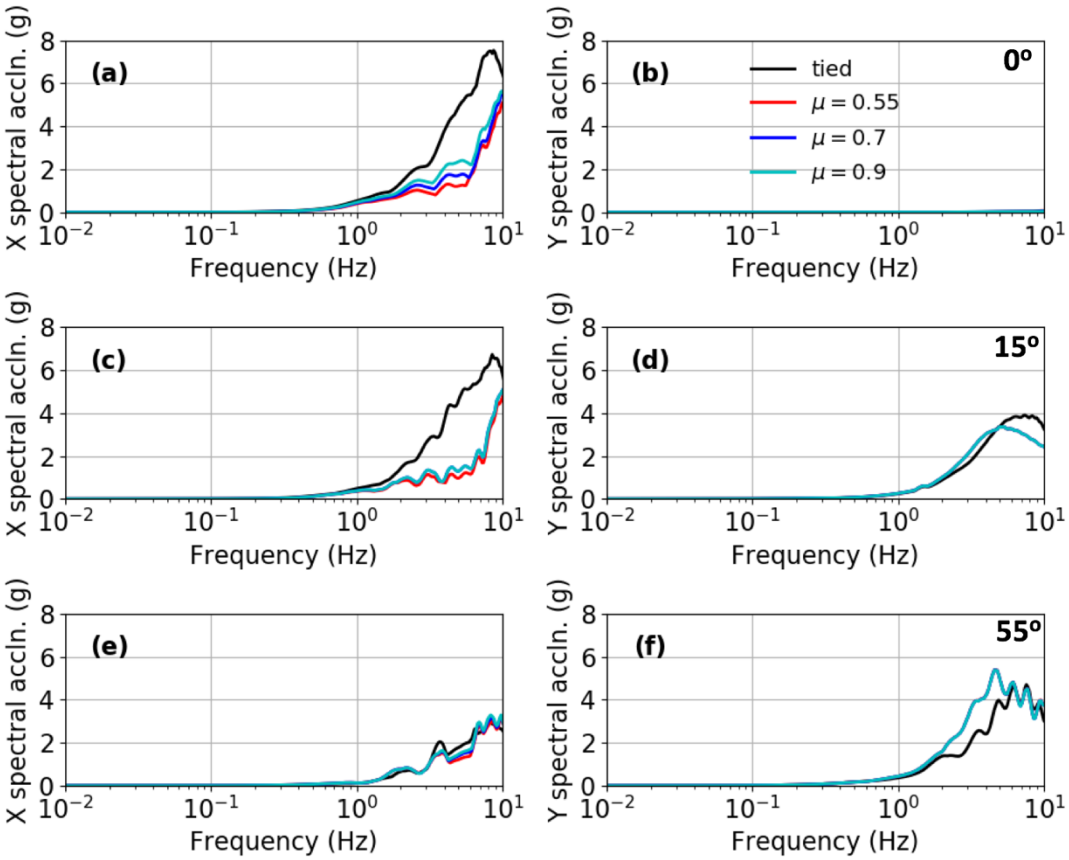

Figure 6. Spectral acceleration of the lumped mass located at 9.8 m from the soil surface as a function of frequency for the three different earthquake fault dip scenarios and the four different soil-structure interface conditions. The left and right column contain horizontal (X) and vertical (Y) spectral accelerations, respectively, and the first, second and third rows contain results for the 0°, 15° and 55° fault dips, respectively. The results for the different interface conditions are shown by the 4 different curves in each subfigure.

CONCLUSION

The effect of geometric nonlinearity on the response of surface-founded structures subjected to inclined seismic waves are examined in this study. An idealized stick-mass model of a nuclear power plant structure connected to a stiff rectangular basemat is considered for this study. This structure is founded on the surface of a linear anelastic homogenous soil domain. The only nonlinearity in the system arises from the sliding, gapping and uplift of the basemat on the soil surface. Three different earthquake fault rupture scenarios are simulated - one generating a vertically propagating shear wave, and others generating inclined SV, P and Rayleigh waves. Four different soil-structure interface conditions are also modelled in this study – tied interface and geometrically nonlinear interface that allows separation and sliding between basemat and the soil, with friction coefficients of 0.55, 0.7 and 0.9.

The results presented in this study indicate that the sliding of the structure on the soil surface is an important damping mechanism that can significantly reduce the horizontal response of the structure for frequencies less than 10 Hz for low seismic wave inclinations angles (0^o and 15^o). Also, modelling separation between the soil and the basement in the vertical direction shows that the natural frequency of the system is quite sensitive to the soil-structure interface conditions. Additionally, for large wave inclinations, the rocking response of the structure can be accentuated when the basemat is not tied to the structure. It is to be noted here that an extreme earthquake scenario is simulated in this study, which has a peak ground velocity of 1.83 m/s and peak ground acceleration around 60 m/s^2, to demonstrate the effects of the geometric nonlinearity. The effects of the geometric nonlinearity would likely be lower, and the results would be closer to the tied interface scenario for smaller earthquake events. Additionally, the basemat in this study is assumed to be located at the soil surface, whereas in reality the foundation of the structure is usually partially embedded in the soil. If the basemat were partially embedded in the soil, there would be additional resistance to sliding that is not considered in this study.

ACKNOWLEDGEMENTS

This project was funded by Idaho National Laboratory's Lab Directed Research Project (#18A12-201FP). The authors would like to thank Dr. Chandrakanth Bolisetti of Idaho National Laboratory for his insightful comments on the manuscript.

REFERENCES

Bielak, J., Loukakis, K., Hisada, Y. and Yoshimura, C. (2003). "Domain Reduction Method for Three-Dimensional Earthquake Modeling in Localized Regions, Part I: Theory," *Bulletin of Seismological Society of America*, 93 (2).

Bolisetti, C., Coleman, J., Talaat, M. and Hashimoto, P. (2015). "Advanced seismic fragility modeling using nonlinear soil-structure interaction analysis.", *INL/EXT-15-36735*, Idaho National Laboratory, Idaho Falls, ID.

Coleman, J., Slaughter, A., Veeraraghavan, S., Bolisetti, C., Numanoglu, O., Spears, R., Hoffman, W. and Kurt, E. (2017). "MASTODON theory manual", *INL/EXT-17-41930*, Idaho National Laboratory.

Luco, J. E. and Wong, H. L. (1982). Response of structures to nonvertically incident seismic waves*, Bulletin of the Seismological Society of America,* 72 (1), 275-302.

Lysmer, J. and Kuhlemeyer, R. L. (1969). Finite Dynamic Model for Infinite Media, *Journal of the Engineering Mechanics Division, Proc. American Society of Civil Engineers*, Vol. 95, EM4, pp. 859-876.

Ostadan, F. (2006). "SASSI2000: A System for Analysis of Soil Structure Interaction - User's Manual." University of California, Berkeley, California.

Thau, S. A. and Umek, A. (1973). Transient response of a buried foundation to antiplane shear waves, *Journal of Applied Mechanics, ASME*, 40, 1061-1066.

Veeraraghavan, S., Bielak, J. and Coleman, J. L. (2017). Effect of inclined waves on deeply embedded nuclear facilities, *Proceedings of the 24th International Conference in Structural Mechanics in Reactor Technology*, Busan, South Korea, August 2017.

Wong, H. L. and J. E. Luco (1978). Dynamic response of rectangular foundations to obliquely incident seismic waves, *Earthquake Engineering and Structural Dynamics*, 6, 3-16.